NATURAL GAS TURBO-EXPANDER SYSTEMS
A Dynamic Simulation Model for Energy and Economic Analyses

by

Giovanni BARONE**, Annamaria BUONOMANO, Francesco CALISE, and Adolfo PALOMBO

Department of Industrial Engineering, University of Naples Federico II, Naples, Italy

Original scientific paper
https://doi.org/10.2298/TSCI180109276B

Natural gas is typically transported for long distances through high pressure pipelines. Such pressure must be reduced before the gas distribution to users. The natural gas lamination process, traditionally adopted for this scope, may determine hydrate formation which may damagingly affect the system operation. Therefore, in order to avoid such circumstance, a suitable gas preheating is required. On the other hand, the available pressure drop can be recovered through a turbo-expansion system in order to provide mechanical energy to drive electricity generators. In this case a higher gas preheating is necessary. This paper presents a detailed simulation model capable to accurately analyse this process as well as the traditional decompression one. Such new model, implemented in a computer tool written in MATLAB, allows one to dynamically assess the energy, economic and environmental performance of these systems, by also taking into account hourly energy prices and weather conditions. Two turbo-expansion system layouts are modelled and simulated. In particular, the gas preheating is obtained by considering two different scenarios: gas-fired heater or solar thermal collectors. Another novelty of the presented dynamic simulation tool is the capability to take into account the time fluctuations of electricity feed-in and purchase tariffs. Finally, a suitable case study relative to a gas decompression station located in South Italy is also presented. Here, a remarkable primary energy savings and avoided CO_2 emissions can be obtained through the examined turbo-expansion systems vs. traditional decompression ones. Results show that the economic profitability of the investigated novel technology depends on the available gas pressure drops and flow rates and on the produced electricity use.

Key words: natural gas *decompression, energy conversion, modelling and simulation*

Introduction

In the past decades, many of the worldwide governments pushed academia and industries in order to investigate new strategies for improving the energy efficiency in all energy sectors. Among all the fossil energy sources available in nature, natural gas (NG) is the second contributing fuel, supplying almost 21.2% of the world primary energy demand [1]. Furthermore, NG is often considered the cleanest available fossil fuel [2].

From the production sites to final users, the supply chain of NG is usually composed of 3-4 hierarchical pressure steps. In European countries, the NG pressure reduction processes are ruled by specific laws and technical regulations [3]. In general, the primary pipelines are

* Corresponding author; e-mail: giovanni.barone@unina.it

adopted for transferring NG over long distances. In such pipelines, often managed by a unique NG distribution company, the gas pressure can often reach 60-70 bar. Such high pressure is basically required in order to limit pipes diameter and to overcome the effects of the occurring pressure losses over the pipeline. Through the secondary pipeline systems, often managed by different local companies [3], the NG is distributed to the final users at a much lower pressure than primary pipelines ones, sometimes less than 1-5 bar. Therefore, a remarkable NG decompression is needed to accomplish with such pressure reduction. To this aim, several NG pressure reduction stations (PRS), based on traditional dissipative Joule-Thompson expansion valves (JTV), are typically used. To avoid the development of undesired hydrate condensation phenomena (in the system conduits at JTV outlet) and to decrease the mechanical stresses of the low pressure pipelines, NG must be suitably pre-heated before the decompression process (mainly through dedicated gas-fired boilers).

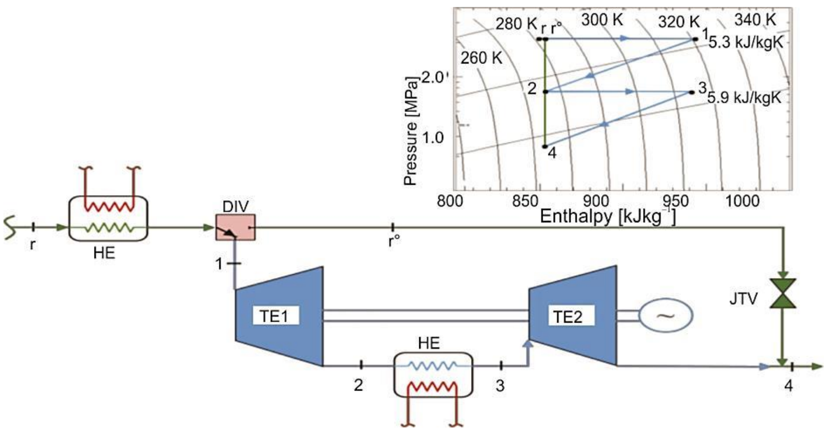

Figure 1. Two-stage TE system; existing/traditional system layout (green line), TE system (blue line) (*for colour image see journal web site*)

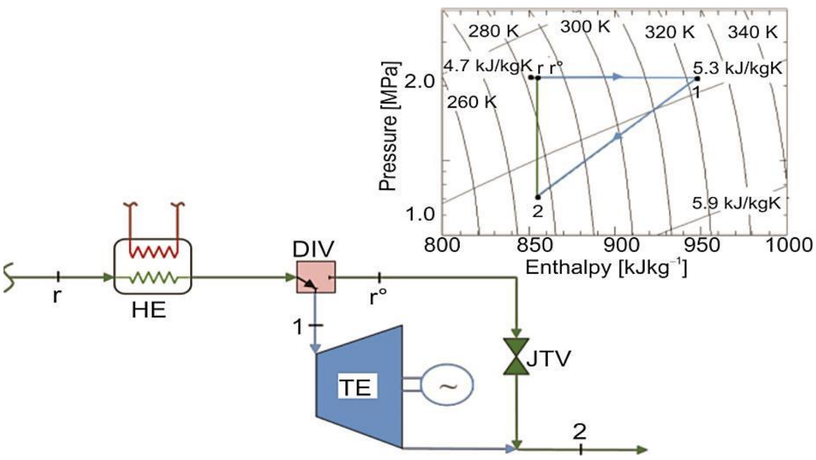

Figure 2. Single-stage TE system coupled in series with an expansion valve; existing/traditional system layout (green line), TE system (blue line)
(*for colour image see journal web site*)

For energy recovery purposes, the pressure drop can be exploited through dynamic or volumetric expanders by obtaining mechanical energy and thus electricity. In fig. 1, a sketch of the typical energy recovery system layout is depicted. Basically, it includes a heat exchanger (HE, linked to a gas-fired heater), a JTV, and a two-stage (in series) turbo-expander (TE1 and TE2). Another system layout can be also considered: the NG can be decompressed through a JTV in series with a single TE, fig. 2. For all these systems, through a suitable diverter (DIV), it is possible to supply in parallel the TE and the standard JTV systems. In addition, in figs. 1 and 2 the thermodynamic routes of the investigated processes are reported in the pressure-enthalpy chart. Note that, such chart and the gas thermodynamic properties used in the carried out simulations are referred to pure CH_4 because of the high percentage of such component contained in NG (which is a natural hydrocarbon gas mixture primarily consisting of CH_4 [4]).

For shifting from traditional NG decompression systems (where just a HE and JTV are included) to such energy recovery systems, a significant initial economic cost must be considered. In addition, NG must be pre-heated before entering the TE to higher temperatures *vs.* ones required by simple JTV systems, usually around 55-85 °C. Thus, in this framework, an additional key problem, limiting the application of TE systems, is represented by the significant operating cost due to the NG pre-heating for preventing the related temperature drop occurring into the TE (that results much higher than that to be considered in the corresponding traditional lamination process).

In order to deal with such issues, the adoption of a suitable dynamic simulation model for the system performance analysis is extremely useful also for assessing the amount of thermal energy that can be obtained through RES (or by cogeneration units) and supplied to the TE systems. This approach can be also exploited to examine the possible technologies and measures to be implemented in the system for maximizing the related energy efficiency.

Many authors have been involved on studies regarding the energy recovery exploitation of available NG pressure drops and the integration of renewable energies as heat source. Among these, only few analyses are focused on developing dynamic simulation models [5-7].

Research effort has been devoted to assess the energy savings potentials of integrated TE systems. Relevant energy savings by such systems were successfully demonstrated by several authors. Pozivill [5] analysed the adoption of a TE system in a NG PRS by using a commercial software (AspenTech's HYSYS process simulator). Here, the investigation of the effects related to a TE isentropic efficiency on both temperature reduction and power generation was carried out.

The same computer tool was also adopted by Unar *et al.* [6] for assessing the electricity production of a PRS located in Pakistan. Borrelli *et al.* [7] investigated the dynamic response of a novel plat configuration and studied the possibility to use low temperature heating sources for pre-heating purpose. Due to the adoption of low temperature thermal energy, the authors carried out a transient analysis for a typical winter scenario in order to assess the potential risk of CH_4-hydrate formation. For this purpose, in this study a transient analysis was carried out for a typical winter scenario. As results, they demonstrated that with a suitable control logic it is possible to use low temperature heat for achieving an average energy saving of about 14% with respect to high temperature system configurations, for a typical winter day. Energy and exergetic aspects of electricity generation from PRS have been investigated by Neseli *et al.* [2]. Here, the authors deal with the feasibility of a TE system by taking into account daily profiles of NG temperatures and pressures. Greeff *et al.* [8] studied the integration of TE into different high pressure exothermic chemical-synthesis processes. Mirandola *et al.* [9] analysed a combined energy recovery system, consisting of a TE coupled to an internal combustion engine cogeneration unit. The system was analysed under full load and part load conditions. The sensitivity of certain design parameters on the plant profitability, such as the duration curve of the NG flow rate, was also assessed. Farzaneh-Gord *et al.* [10] investigated the feasibility of coupling a solar system to traditional NG PRS. A numerical method, based on mass and energy balance, was developed and applied to a case study related to a system located in city of Akand City, Iran. The analysis was carried out by considering an hourly analysis of solar collectors' operation while NG pressure drop parameters were considered in steady state. Results showed a potential reduction of 11.3% of fuel consumption and a payback period of 3.5 years. Through the same approach, the same authors investigated the use of a vertical geothermal HE as thermal source [11, 12]. Here, part of the heat required to preheat the NG is obtained by means of a vertical ground-coupled heat pump: the analysis revealed that the yearly fuel saving potential of such system could be more than 45%, with a discounted payback period of about six years. Badami *et al.* [13] analysed the energy efficiency for four possible operation strategies of an oil cogeneration unit coupled to a double-stage TE system. Jelodar *et al.* [14] investigated the dynamics of TE systems. They developed a comprehensive model of a TE system and the related components. In particular, they focused on the system nozzle angle and turbine. The results demonstrated the importance of the control system on the turbine operation and output gas pressure.

A lack of knowledge is detected in the aforementioned literature review. Specifically, despite of some studies in which the dynamic response of TE system is investigated, none of the results were presented concerning the energy, economic and environmental performance analysis of NG TE systems through the use of a dynamic simulation model capable to take into account the time fluctuations in the day hours of:

- occurring gas pressure drops and flow rates,
- tariffs for purchasing the NG and selling the produced electricity (by national rules or laws), and
- weather conditions (including the solar radiation eventually exploited for the NG preheating).

By adopting a dynamic analysis approach, accurate investigations for assessing the system economic convenience can be carried out. For this reason, a new in-house dynamic performance analysis simulation model was purposely developed, with the aim to optimize the system design too. Through such tool, energy, economic and environmental investigations can be easily carried out by simply taking into account hourly data related to NG temperatures, pressure drops, and flow rates measured and logged at existing traditional decompression stations. An additional simulation tool takes into account for the gas heating the thermal energy obtained by suitable solar thermal collectors – STC (or optionally supplied by cogeneration plants). Therefore, different simulation models were developed for all the above reported TE system layouts (figs. 1 and 2). All such models were implemented in a suitable computer code written in MATLAB.

In order to show the potentiality of the presented computer simulation tool, two novel case studies are developed. They refer to a NG decompression station located in South Italy for residential uses. By the calculated results, interesting guidelines useful to designers and practitioners are obtained.

Simulation model

In this section, the developed dynamic simulation model for the performance analysis of the energy recovery by the NG decompression is described. The model is capable to calculate the electricity production, the NG heating demand, and the overall system energy efficiency. Economic system performance can be also assessed. The developed model is implemented in a computer code, written in MATLAB environment, that can be operated starting from real measured data. All the results can be computed hour by hour over different time periods (week, month, year). For all the above presented system layouts (figs. 1 and 2), the thermal energy for the NG heating is supposed to be alternatively supplied by:

– a gas-fired boiler,
– a co-generation unit, and
– a STC field.

In detail, the model consists of a quasi steady-state calculation procedure based on the solution of mass and energy balances coupled to suitable design algorithms and system datasheets provided by the system components. Hourly code inputs are: NG flow rate, $\dot{m}$, inlet pressure, p_{inlet}, and temperature, t_{inlet}, outlet pressure, p_{outlet}. Hourly results of the calculations are: electricity production, required temperature and thermal energy demand for NG heating, temperature of the decompressed NG, main system components and whole system energy efficiencies. By the code the NG thermodynamic properties are calculated by considering the NG as fully composed by CH_4 for which temperature-dependent specific heats are taken into account [4]. Density and lower heating value are variable as a function of temperature and pressure.

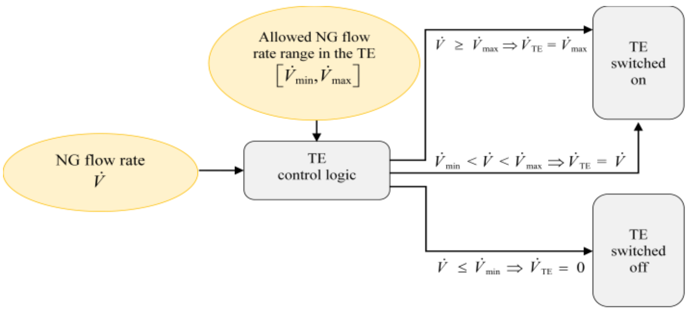

Figure 3. The TE control logic as a function of the NG flow rate to be decompressed

For all the considered system layouts, the TE running regime depends on the NG flow rate to be decompressed (variable hour by hour as a function of the user demand). From this point of view the adopted control logic is summarised in fig. 3. Obviously, the achievable TE working hours depend on the related minimum and maximum allowed flow rate range. Specifically, the TE is activated only when the inlet flow rate is higher than $\dot{V}_{\mathrm{min}}$ (conversely, the NG is decompressed by the JTV only). When the NG flow rate is higher than $\dot{V}_{\mathrm{max}}$, the one decompressed by TE ($\dot{V}_{\mathrm{TE}}$) is equal to $\dot{V}_{\mathrm{max}}$ whilst the residual flow rate ($\dot{V}_{\mathrm{exaust}}$) is laminated.

Thermodynamic analysis

The system hourly operating conditions are assumed to be obtained through several measurements at PRS, including the NG mass-flow rate required by the users and the related pressure ratio. By means of such data and through the manufacturers' operating map of the TE, the related isentropic efficiency can be calculated. For each considered system layout, the thermodynamic state of the TE outlet stream can be assessed by the related enthalpy, h_2 [kJkg^{-1}], calculated by:

$$\eta_{\text{isTES1}} = \frac{h_1 - h_2}{h_1 - h_{2\text{is}}} \quad \text{and} \quad \eta_{\text{isTES2}} = \frac{h_3 - h_4}{h_3 - h_{4\text{is}}}$$
$$\eta_{\text{isTEV}} = \frac{h_1 - h_2}{h_1 - h_{2\text{is}}} \tag{1}$$

where η_{isTES1} and η_{isTES2} are related to the system layout with two TE in series, fig. 1, η_{isTEV} is referred to the system where the NG is decompressed through a valve and a TE in series, fig. 2.

For such system configurations, the related electric power, P_{el} [kW], are calculated hour by hour:

$$P_{\text{elTES}} = \dot{m}\left[(h_1 - h_2) + (h_3 - h_4)\right]\eta_{\text{m}}\eta_{\text{g}}$$
$$P_{\text{elTEV}} = \dot{m}(h_1 - h_2)\eta_{\text{m}}\eta_{\text{g}} \tag{2}$$

where $\dot{m}$ [kgs^{-1}] is the hourly turbo-expanded NG flow rate, η_{m} – the TE mechanical efficiency, η_{g} – the efficiency of the electric generator. In the presented model, η_{m} and η_{g} are assumed equal to 0.90 and 0.92, respectively. By the simulation code the option of NG heating obtained through a suitable cogeneration system is also taken into account. In this case, the total electric power production is considered as sum of that obtained through eq. (2) and the one achieved by the cogeneration system:

$$P_{\text{elCOG}} = \eta_{\text{elCOG}} E_{\text{pCOG}} \tag{3}$$

where η_{elCOG} is the co-generation electricity efficiency and E_{pCOG} [kW] is the primary thermal power supplied to the cogeneration system.

The heating power that must be supplied to the NG for pre-heating purposes before the TE decompression process for all the aforementioned system layouts (see figs. 1 and 2) is calculated:

$$\dot{Q}_{\text{TES}} = \dot{m}\left[(h_1 - h_{\text{r}}) + (h_3 - h_2)\right]$$
$$\dot{Q}_{\text{TEV}} = \dot{m}(h_1 - h_{\text{r}_0}) \tag{4}$$

In all the cases, the net thermal power $\dot{Q}_{\text{net}}$ required to the NG preheating [kW] (excluding the rate required for warming up the NG for the simple lamination valve decompression) is calculated:

$$\dot{Q}_{\text{net}} = \dot{m}(h_{\text{r*}} - h_{\text{r}}) \tag{5}$$

Note that in the developed model such thermal power can be supplied also by a STC field. Obviously, in this case the obtained energy saving depends on the weather conditions (here, the gas-fired heater is adopted only as backup system).

The yearly primary energy saving (*PES*), is calculated:

$$PES = \frac{E_{\text{el}}}{\eta_{\text{el}}^{\text{ref}}} - E_{\text{p}} \tag{6}$$

where $\eta_{\text{el}}^{\text{ref}}$ is national thermoelectric efficiency, E_{el} [kWh$_{\text{e}}$y^{-1}] – the yearly electricity produced by the TE system (such result is obtained summing the hourly calculated ones), E_{p} [kWh$_{\text{p}}$y^{-1}]

– the net primary energy consumed by TE (for the NG heating from r^* to 1, *e. g.* see fig. 1). Note that E_{el} and E_p are obtained by summing the related hourly calculated results.

In case of traditional gas-fired heater, solar collector or co-generative unit, E_p is calculated respectively by the following equations:

$$E_p = \frac{\sum_{i=1}^{WH}[\dot{m}(i)\Delta h(i)]\theta}{\eta_{heater}} \quad \text{(for gas-fired heater)}$$
$$E_p = \frac{\dot{Q}_{int}}{\eta_{heater}} \quad \text{(for solar thermal collector)} \tag{7}$$
$$E_p = \frac{\dot{Q}}{\eta_{thermal}\varepsilon_{HE}} \quad \text{(for co-generative unit)}$$

where WH is the number of yearly hours (with θ = 1 hour) in which the TE is switched on, η_{heater} – the efficiency of the gas-fired heater, $\dot{Q}_{int}$ [kWh$_t$y^{-1}] – the thermal energy (necessary to the solar collectors' system heating integration) to be supplied through the adopted backup system (auxiliary gas-fired heater), $\eta_{thermal}$ – the efficiency of the cogenerative unit, and η_{HE} – the efficiency of the gas preheating HE.

The global yearly efficiency of the whole system is assessed:

$$F_{glob} = \frac{E_{el}}{E_p} \tag{8}$$

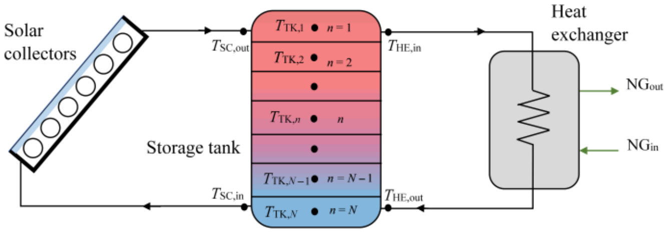

Figure 4. A schematic diagram of the solar thermal system

Solar thermal system

The solar thermal system, fig. 4, consists of a stratified water storage tank coupled to a STC field and to the HE for the NG preheating.

In order to take into account stratification effects, the tank is subdivided in N fully-mixed equal sub-volumes or nodes, fig. 4, where flow streams from the solar field and toward the load, respectively, enter and exit at fixed positions. By taking into account steady-state conditions, for each n-th sub-volume and in each time step, t, the energy balance including the heat losses toward the outdoor ambient and the heat delivered from the collector array and supplied to the plant (*i. e.* HE) is calculated according to:

$$C_{TK,n}\frac{\partial T_{TK,n}}{dt} = \dot{m}_{SC}c_p(T_{TK,n-1} - T_{TK,n}) + \dot{m}_{HE}c_p(T_{TK,n+1} - T_{TK,n}) - UA_{ext}(T_{TK,n} - T_{amb}) + \ldots$$
$$\ldots + UA_{int}\left[\gamma^a(T_{TK,n-1} - T_{TK,n}) + \gamma^b(T_{TK,n+1} - T_{TK,n})\right] \tag{9}$$

where T_{TK} [K] is the node temperature, C_{TK} [kWK^{-1}] – the capacity of the sub-volumes, c_p [kJkg^{-1}K^{-1}] – the specific heat of water, $\dot{m}_{SC}$ [kgs^{-1}] – the solar collectors mass-flow rate, $\dot{m}_{HE}$ [kgs^{-1}] – heat recovery exchanger mass-flow rate, and UA [WK^{-1}] are the external and internal conductances defined in tab. 1. Note that for n = 1 and n = N, $T_{TK,n-1}$ and $T_{TK,n+1}$ are equal to the STC $T_{SC,out}$ and to the HE $T_{HE,out}$ outlet water temperatures, respectively, whereas their

Table 1. Calculated thermal conductances

Conductance	Equation
$(UA)_{\text{int}}$ [WK^{-1}]	$\dfrac{k_{\text{w}}}{s_{\text{w}}}A_{\text{b}}$
$(UA)_{\text{ext}}$ [WK^{-1}]	$\dfrac{k_{\text{tank}}}{s_{\text{tank}}}A_{\text{b}}+\dfrac{k_{\text{tank}}}{s_{\text{tank}}}A_{\text{l}}$ for n = 1, N
	$\dfrac{k_{\text{tank}}}{s_{\text{tank}}}A_{\text{l}}$ for n = 2,…, N − 1

corresponding inlet water temperatures, $T_{\text{SC,in}}$ and $T_{\text{HE,in}}$ are equal to $T_{\text{TK,N}}$ and $T_{\text{TK,1}}$, fig. 4. Note that for such temperature boundary nodes, γ^{a} (for n = 1) and γ^{b} (for n = N) are set to zero (being equal to 1 otherwise). In tab. 1, k_{tank} and k_{w} [Wm^{-1}K^{-1}] are the thermal conductivity of the tank and the water, s_{tank} and s_{w} [m] are the thickness of the tank envelope and the control volume, and A_{l} and A_{b} [m^2] are the lateral and base surface area of the control volume. Note that a cylindrical tank is taken into account.

In order to assess the solar collectors' inlet and outlet temperatures, $T_{\text{SC,out}}$ and $T_{\text{SC,in}}$, it is also necessary to calculate the solar thermal production, $\dot{Q}_{\text{SC}}$:

$$\dot{Q}_{\text{SC}} = \eta_{\text{SC}} I_{\text{sol}} A_{\text{SC}} = \dot{m}_{\text{SC}} c_{\text{p}} (T_{\text{SC,out}} - T_{\text{SC,in}}) \tag{10}$$

where η_{SC} is the STC efficiency, calculated:

$$\eta_{\text{SC}} = \eta_0 IAM_{\text{b}} + \eta_0 IAM_{\text{d}} - a_1 \frac{T_{\text{m}} - T_{\text{amb}}}{I_{\text{sol}}} - a_2 \frac{(T_{\text{m}} - T_{\text{amb}})^2}{I_{\text{sol}}} \tag{11}$$

where T_{m} [K] is STC average temperature, *IAM* – the incidence angle modifier of STC, and η_0, a_1 and a_2 are the coefficients of a polynomial curve of the η_{SC}, estimated through simulations and indoor-outdoor tests performed according to EN 12975 and EN 12976 [15].

The heat recovery exchanger is a shell and tube HE with water as intermediate fluid; in order to calculate $T_{\text{HE,out}}$ and $T_{\text{HE,in}}$, the ε-NTU methodology is taken into account [16]. The thermal power supplied to NG flow rate by auxiliary boiler, $\dot{Q}_{\text{int}}$ [kW], is calculated by:

$$\dot{Q}_{\text{int}} = \dot{m}_{\text{gas,int}} c_p (T_1 - T_{\text{NG,out}}) \tag{12}$$

where $\dot{m}_{\text{gas,int}}$ [kgs^{-1}] is the NG flow rate supplied to auxiliary boiler, and T_1 [K] is the TE inlet temperature, fig. 1. Finally, note that auxiliary electricity required to drive the water pump is neglected.

Environmental analysis

For all the innovative considered TE system layouts as well as for the traditional decompression system, the primary energy related to the NG consumption necessary for the NG preheating process is calculated:

$$E_{\text{p}} = \sum_{i=1}^{\text{WH}} \left[\dot{V}_{\text{gas}}(i) LHV \right] \theta \tag{13}$$

where $\dot{V}_{\text{gas}}$ [Sm^{3}h^{-1}] is hourly NG flow rate burned in the gas-fired heater (before entering the TE in the innovative systems or JTV in the traditional one) and *LHV* [kWhS^{-1}m^{-3}] – the NG lower heating value. The CO_2 emission to the atmosphere due to E_{p} for the same amount of produced in all the proposed system (superscript *pro*) and in the reference one (superscript *ref*, obtained by the national thermoelectric system) are calculated:

$$M_{CO_2}^{pro} = f_{NG,H} E_p$$
$$M_{CO_2}^{pro} = f_{NG,COG} \ \eta_{tCOG} \ E_{pCOG} \tag{14}$$
$$M_{CO_2}^{ref} = f_{el} E_{el}$$

where $f_{NG,H}$ $[kg_{CO_2} Sm^{-3}]$, $f_{NG,COG}$ $[kg_{CO_2} Sm^{-3}]$, and f_{el} $[kg_{CO_2} kWh_e^{-1}]$ are the CO_2 emission factors related to the NG combustion in the gas-fired heater, NG consumption in the cogeneration unit and electricity production through the national thermoelectric system, respectively.

Economic analysis

In order to investigate the economic feasibility of the investigated TE systems, two different scenarios relative to the produced electricity are considered, such as: selling to the national grid and self-consumption. In both the cases, for a detailed economic analysis, the developed model takes into account the hourly electricity selling and purchase tariffs as well as the incentives provided by national legislations. Often, self-consumption is much more convenient than selling because of the spread between purchase and selling prices. In case of self-consumption, electricity could be utilized to satisfy the electricity needs for internal use of the NG distribution company, but this chance is not always available due to the occurring long distances between PRS and users or the possible total absence of electricity demand of the company. In these cases, the unique chance is the produced electricity selling to the grid.

Regarding the electricity selling to the grid an hourly price fluctuation can be imposed by the market. As an example, in Italy in order to achieve the balance between electricity demand and supply a national single price (*NSP*) variable hour by hour is imposed. Note that, the Italian *NSP* is highly hourly variable, fig. 5.

By the presented dynamic simulation code, this aspect is accurately taken into consideration. It is worth noting that different models about NG turbo-expansion available in literature take into account only a yearly, monthly or daily average electricity price.

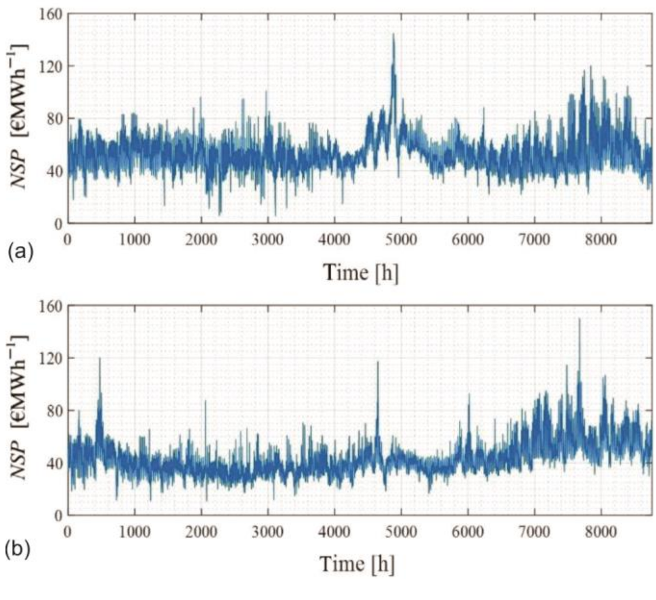

Figure 5. The *NSP* hourly fluctuation for 2015 year (a) and 2016 year (b)

In Italy, some economic incentives available for energy efficiency can be exploited for TE and solar systems. For the TE electricity production in Italy the tradable white certificates (TWC) can be obtained. On one hand, electricity and NG distributors are obliged to reach annual quantitative targets for PES (1 TWC = 1 saved TOE). On the other hand, TWC can be sold on a dedicated market. The number of TWC yearly achieved through a TE plant can be calculated:

$$\text{TWC} = \tau \, 0.1045 E_{el} \cdot 10^{-3} \tag{15}$$

where τ = 0.36 is a coefficient of

durability. In Italy, specific incentives are available also for STC [17]. Specifically, such incentive, IN_{tot}, achievable as a function of the related estimated produced thermal energy per square meter Q_u [$kWh_t y^{-1} m^{-2}$], can be calculated:

$$IN_{tot} = Q_u C_i S_i \tag{16}$$

where C_i is a coefficient depending on the use of the produced heat, S_i [m^2] is the installed gross surface area of the solar collectors' field.

Case study

The developed case study refers to a PRS located in South Italy where presently only a simple JTV decompression system is operating for reducing the NG pressure to a constant value of 250 kPa. In order to carry out a suitable energy and economic feasibility analysis of the systems depicted in figs. 1 and 2, hourly measured NG flow rates, upstream pressures and higher heating values are taken into account, whereas the hourly Metronome weather data file of the climate zone under exam is considered. Note that, for the selected case study a typical daily NG demand for residential user, fig. 6, is taken into account. In addition, by examining the upstream pressure measurements, high seasonal fluctuations and remarkable expansion ratios occur, $7 < \beta < 10$, fig. 7.

For this reason, the use of a single TE to perform all the pressure drop is not recommended, therefore TES, fig. 1, and TEV, fig. 2, systems are investigated. Regarding the occurring NG flow rates, quite low values are detected since the examined PRS is deputed to the NG supply of a rather little residential community, fig. 7. For such operating conditions, a TES and a TEV layout with an electricity power of 2 × 80 and 160 kW_e were taken into consideration, respectively. The features of the considered TE are reported in tab. 2.

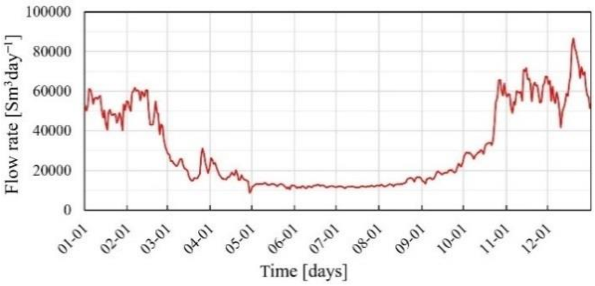

Figure 6. Daily NG demand

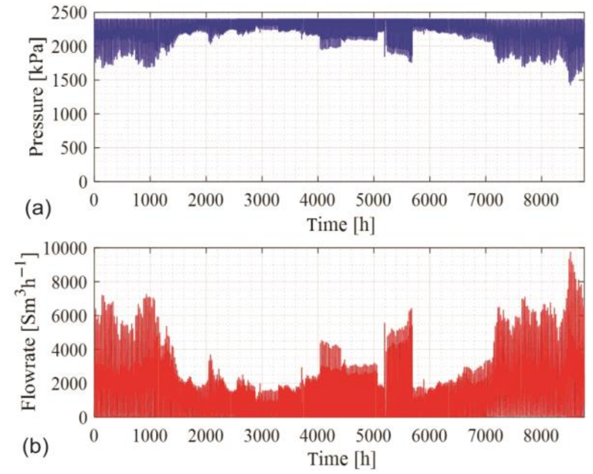

Figure 7. Time history of NG upstream pressures (a) and flow rates (b)

Table 2. The TE features (Turbinde [18])

Model		2MTG160 (two-stages)	MTG 60
	Units	Value	
Minimum flow rate	Sm^3h^{-1}	1000	1400
Maximum flow rate	Sm^3h^{-1}	4500	7500
Inlet pressure	bar	60-24	24
Outlet pressure	bar	24-2.5	2.5
Minimum inlet temperature	°C	−40	−40
Maximum inlet temperature	°C	100	100
Net electricity power	kW_e	2 × 80	160
Cost	k€	600	400

In order to assess the energy performance of both such system layouts in different working conditions, a simplified characteristic curve (referred to MTG 160) is implemented in the simulation model, fig. 8. This curve (and the related obtained equation) is based on experimental data and it is referred to the expansion ratio β = 2.4 and to the TE inlet temperature equal to 350 K.

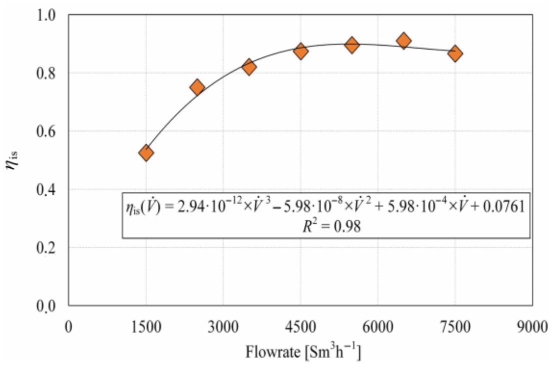

Figure 8. Characteristic curve of MTG 160

A shell and tube HE for the NG preheating with a surface of 100 m^2 and a *U*-value equal to 250 W/m^2K is considered. Note that, during many summer hours and winter nights the flow rates are considerably reduced leading to many empty hours in which no flow rates are detected. For all these reasons, a rather low number of TE operating hours are expected. Due to this highly intermittent behaviour the adoption of a cogeneration unit for preheating purposes is not recommended (such technology is competitive only in case of stable and high thermal energy demands). Therefore, only a gas-fired heater and a STC field are simulated as thermal source for the NG preheating. Regarding the gas-fired heater the related power and efficiency (η_{heater}) are equal to 400 kW and 0.90, respectively. Concerning the solar collectors as thermal source, a number of 28 (high vacuum, high temperature) flat-plate panels, for a total of 54.6 m^2, with a south-facing surface and a tilted angle of 45° were selected. The solar field is coupled to a 1500 L water heat storage tank. The features of the considered STC are reported in tab. 3 and fig. 9, respectively.

Table 3. The STC features (TVP solar, MT-power)

	Unit	Value
Length × height	m	2.00 × 0.96
Gross area	m^2	1.95
Aperture area	m^2	1.84
Weight	kg	52
Volume of HT fluid	L	1.3
Cost	€m^{-2}	500
Heat absorber-pipe	Al sheet + Cu pipe	
Absorber coating	Alanod Mirotherm 1300R	
Back-plate	441 stainless steel	
Glass coating	Single-side anti-reflective (interior face)	
Operating conditions		
Stagnation temperature	°C	310
Maximum operating pressure	bar	16
η_0	–	0.759
a_1	$Wm^{-2}K^{-1}$	0.508
a_2	$Wm^{-2}K^{-2}$	0.007
H_2O pressure drop	kPa	0.7

The following additional assumptions are taken into account in this case study: the NG preheating is hour by hour arranged in order to obtain an outlet temperature from TE higher than −5 °C, the maximum NG preheating temperature is set at 50 °C, the heat storage tank water temperature is set to be always lower than 100 °C, the thermoelectric system efficiency (η_{el}^{ref}, referred to the Italian system) is equal to 0.46, the NG *LHV* is equal to 9.61 kWh/Sm^3, in the economic analysis the electricity unitary price is 0.18 €/kWh_e in case of self-consuming strategy whilst it follows hour by hour the 2016 *NSP* in case of selling one, for the selected TE electricity power the value of 1 TWC is equal about to 100 € [17].

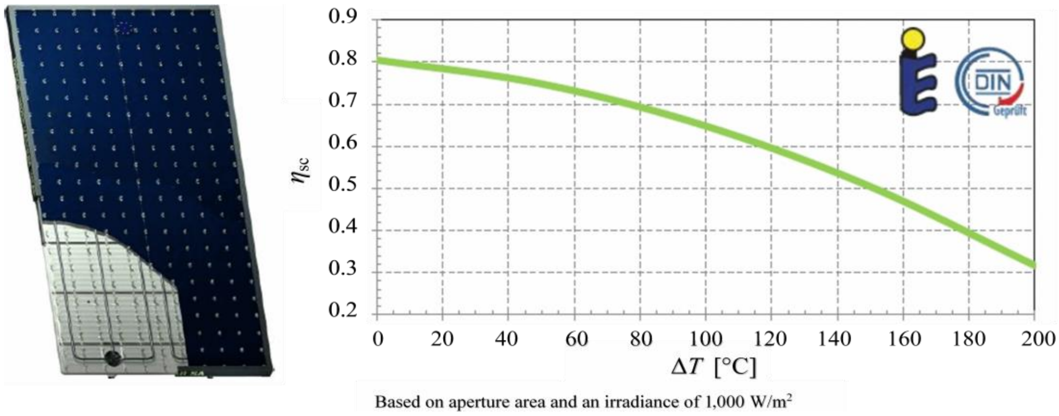

Figure 9. Solar collector efficiency curve (TVP solar, MT-power [19])

Result and discussion

For both the examined system configurations, the rather frequent flow rate fluctuation under the minimum related limit dramatically affected the calculated TE performance. Specifically, the obtained TE working period resulted of 3297 and 4051 hours per year for TEV and TES layout, respectively. During these hours, a high NG flow rate variation (due to the occurring user demand) is detected, as it is reported in fig. 10. Here, for the TEV layout, the time history (over 3297 TE running hours) of the TE isentropic efficiencies corresponding to the fluctuating NG flow rate are also shown (in the whole year they range from 0.52 to 0.92). In this figure, for each hourly timestep, two different marker types are shown: the black one is referred to the NG flow rate exploited in the TE, whereas the coloured ones are related to the TE isentropic efficiency (blue plots are referred to low efficiencies, whereas red ones to high ones). Note that, according to the characteristic curve depicted in fig. 7, the higher the flow rate the higher the isentropic efficiency. By fig. 10 it is clearly visible that in almost all the yearly running hours different TE speed regimes (and correspondently a wide range of isoentropic efficiencies) are observed. Note that, in winter high NG flow rates and TE efficiencies are detected *vs.* spring and fall ones. In summer, rather high NG hourly flow rates are detected because of the occurring seasonal building use of the selected case study.

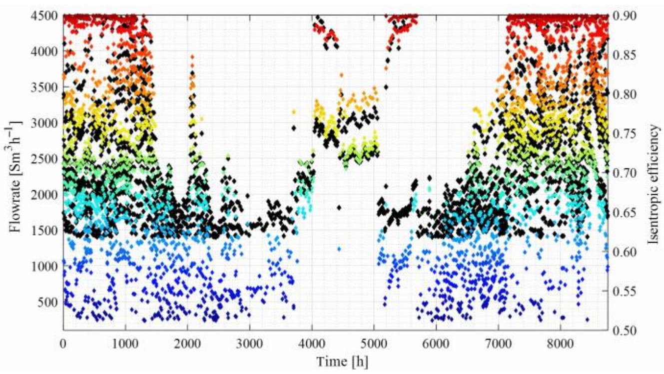

Figure 10. The TEV system layout: time history of NG flow rate and TE isentropic efficiency (*for colour image see journal web site*)

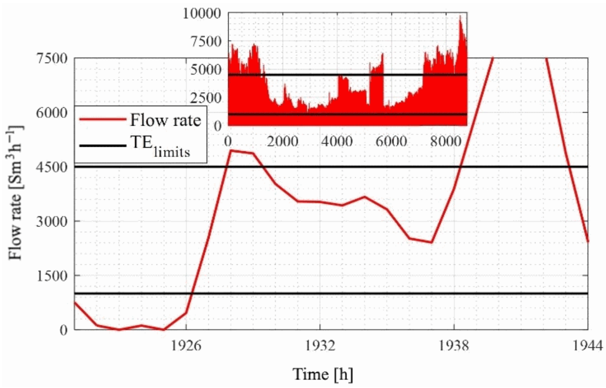

Figure 11. The TES system layout; time history of NG flow rate (blue line) for a spring sample day (March 21th)
(*for colour image see journal web site*)

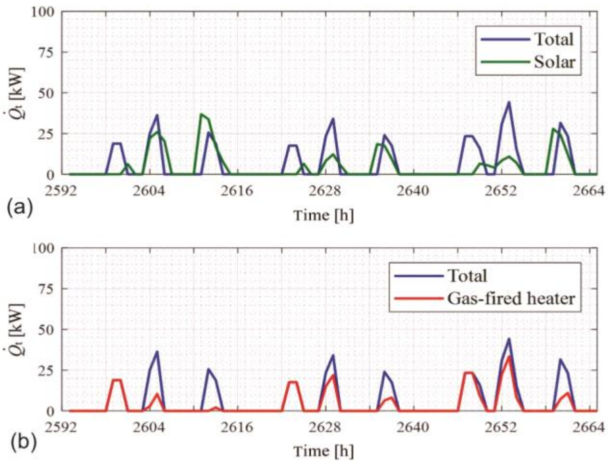

Figure 12. The TES system layout; time history of the thermal power for NG heating obtained by the solar energy (a) and by the backup gas-fired heater (b) for three springs sample days (April 20th-22th)

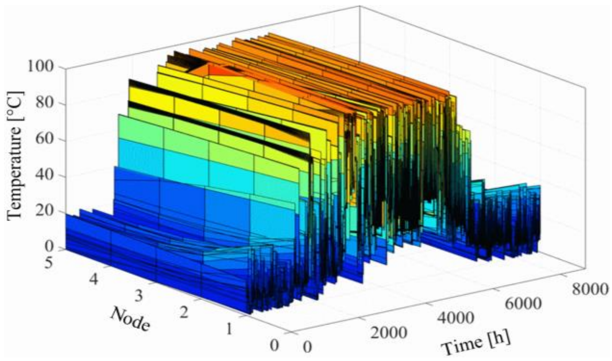

Figure 13. The TES system layout: time history of the tank hot water temperatures (node by node)
(*for colour image see journal web site*)

Note that, despite of such high flow rates the corresponding summer NG demands are obviously low as it is clearly visible in fig. 6.

In the following, because of the higher working hours of the TES system layout *vs.* TEV one, details of the obtained results of the TES configuration are discussed. Specifically, fig. 11 shows the hourly NG flow rate available for the TE process for a spring sample day compared to the related TE minimum and maximum limits, tab. 2. Obviously, for occurring NG flow rates lower than the minimum allowed one, the TE is deactivated whilst for flow rates higher than the maximum one the excess is laminated by means of the backup JTV.

Figure 12 shows time history of the thermal power for NG heating for three spring sample days. Here, it is possible to observe the amount of the heating demand supplied by solar energy, fig. 12(a), and the corresponding one provided by the backup gas-fired heater, fig. 12(b). When the NG heating demand is lower than the solar thermal energy production, it is possible to collect the produced solar heat in the water storage tank, fig. 4.

The stored heat can be exploited during the hours in which the solar radiation is unavailable. For the entire year, according to eq. (9) the time history of the tank hot water temperatures (node by node) are shown in fig. 13. By such graph it is qualitatively visible the significant contribution of the solar energy to the NG preheating. Note that, averagely high temperatures are often obtained in the stratified heat storage tank, in this case discretized through five nodes.

In fig. 14, the time history of the tank top node temperature, NG flow rate, and upstream pressure for three summer sample days are reported.

By this figure it is possible to observe that the higher the NG flow rates, the lower the NG upstream pressures and the lower the water temperature in the heat storage tank.

In fig. 15, the monthly thermal energy demand for the NG heating, heat supplied by solar collectors, and heat integration by the backup gas-fired heater are shown. By such figure it is possible to detect that, during summer and autumn periods solar energy determines a significant reduction of the thermal energy supplied by the heater. During all the year, a monthly energy saving ranging from 10 to 86% is achieved.

In fig. 16, for both TES and TEV system layouts, the monthly electricity production is shown. As expected, due to the entire pressure drop exploitation obtained through the TES system configuration a higher electricity production is always achieved.

In tab. 4, the main yearly energy results are reported for both TES and TEV system layouts. A total NG flow rate of $11.28 \cdot 10^6$ Sm^3/y are decompressed at the considered PRS. As previously reported, because of the discussed constraints, the yearly working hours of TES and TEV system layouts are 3297 and 4051, respectively. The NG flow rates decompressed by TES and TEV system layouts are $9.74 \cdot 10^6$ and $9.32 \cdot 10^6$ Sm^3/y, respectively. Such results correspond about to 86 and 83% of the total flow rate at PRS, respectively.

A yearly electricity production of about 337 and 180 MWh_e per year

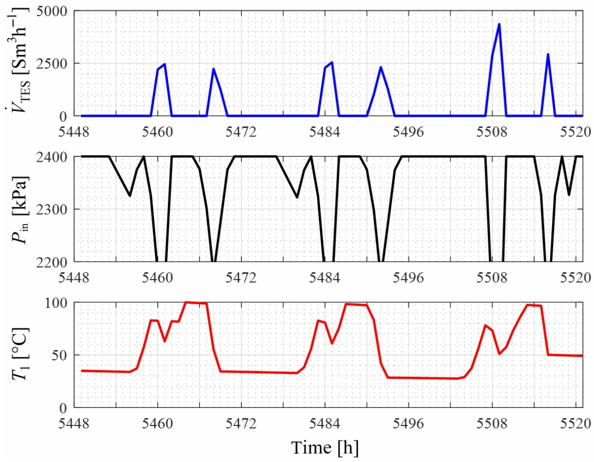

Figure 14. The TES system layout: time history of the tank top node temperature, NG flow rate and upstream pressure for three summer sample days (August 14th-16th) (*for colour image see journal web site*)

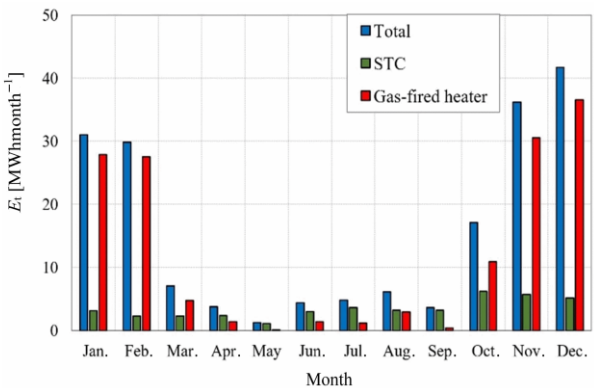

Figure 15. The TES system layout: monthly thermal energy requirement for NG heating

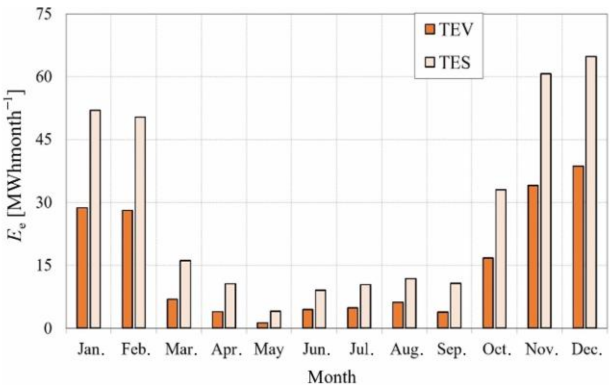

Figure 16. The TES and TEV system layouts: monthly electricity production

Table 4. Yearly energy results for TES and TEV system layouts (constraint for the TE running: minimum allowed NG flow rate)

	Unit	TES	TEV
TE working hours	hy^{-1}	4051	3297
Flow rate at PRS	Sm^3y^{-1}	$11.28 \cdot 10^6$	
Flow rate decompressed by TE	Sm^3y^{-1}	$9.74 \cdot 10^6$	$9.32 \cdot 10^6$
Percentage of flow rate decompressed by TE	%	86.3	82.6
Electricity production	MWh_ey^{-1}	336.8	179.5
Thermal energy demand	MWh_ty^{-1}	377.3	180.8
Primary energy demand	$MWhy^{-1}$	419.3	186.8
Net primary energy demand (with STC)	$MWhy^{-1}$	349.5	158.2
Share of renewable energy	%	16	15
PES	$MWhy^{-1}$	375.3^{*}-312.9^{**}	228.2^{*}-182.8^{**}
Percentage of *PES*	%	52^{*}-43^{**}	59^{*}-47^{**}
Avoided CO_2	$t_{CO_2}y^{-1}$	75.6^{*}-65.1^{**}	45.8^{*}-36.1^{**}

* with STC
** with gas-fired heater

are obtained by TES and TEV system layouts, respectively. The primary energy requirements for NG preheating are about 419 and 187 MWh per year, respectively. By the adoption of the considered STC such demands decrease to 350 and 158 MWh per year, respectively. Referring to the share of renewable energy, a rather small weight on the total primary energy demand (16-15%, respectively for the two examined system layouts) is detected. This rather unsatisfactory result is due to different reasons:

– the NG demand follows a strong seasonality, in fact the higher thermal energy demands (for the required NG heating) occur during the winter season, as it can be seen in fig. 17 for the TES system layout,
– the investigated PRS feeds residential users, so the NG demand follows users' needs that vary significantly day-by-day reaching a peak during hours in which the solar radiation is scarce or null; this occurrence is clearly visible in figs. 17 and 18 that shows the time history (for three summer, winter and mid-season sample days) of the thermal power:
  - required for the NG heating, and
  - supplied by the solar collectors, and
– solar system capacity should be optimized for the considered NG heating purpose (*e. g.* heat storage tank volume, heat transfer fluid temperatures, *etc.*); such target will be obtained in a next future paper.

Remarkable PES are obtained *vs.* traditional system in which the same amount of electricity is obtained by the national thermoelectric system. Specifically, PES range between 43 and 59%. Regarding the avoided CO_2, interesting results are achieved. In particular, the carried-out calculation shows that the avoided CO_2 emissions range about from 36 to 75.6 t_{CO_2} per year.

At last, a suitable economic analysis is carried out by taking into account two different strategies in which the produced electricity is:

– self-consumed by the NG distribution a company, and
– sold to the national grid.

For the selling strategy, the TE working hours calculated by the presented simulation code depends on the occurring electricity selling prices as well. In fig. 19, for a winter sample day, the effect of this running constraint (additional to the above described one related to the minimum TE allowed flow rate) is shown. During the hours in which the selling price is lower than a selected minimum threshold (in this case study NSP_{min} is set to 0.039 €/kWh), the TE system is switched off (in order to avoid operating costs higher than the obtainable economic proceed). Note that, in all the above reported results such TE running constraint is not taken into account. The simulation results related to the system energy analysis, taking into account both the minimum allowed NG flow rate and NSP, are reported in tab. 5. Obviously, a reduction of the TE working hours and the related produced electricity is detected *vs.* the results reported in tab. 4. In this case, PES range between 42 and 57%.

In tab. 6, the results of the carried out economic analysis are reported. Here, the columns named *sell* and *self* are referred to the selling and self-consuming strategies, respectively. Note that, in tab. 6, the first column takes into account the NSP_{min} of 0.039 €/kWh under which the TE system is switched off.

All the reported economic results take into account the TWC incentives in order to achieve the maximum economic benefit. Note that, a high number of TWC can be obtained for all the investigated configurations (from 53 to 118 TWC/y). Further incentives can be achieved in case of solar thermal panels adoption (as thermal source). In case of self-consuming strategy, the obtained economic results are always much better than the electricity selling ones because of the higher difference between the electricity unitary cost vs. the occurring *NSP* (tab. 6). Note that, the initial costs of the TE devices are still today rather high. Therefore, the obtained SPB periods are averagely long. While for self-consuming strategies they resulted always less than 10 years, in case of electricity selling the obtained SPB surpass 33 years. Such results negatively affect the TE convenience, limiting the TE energy recovery during certain periods of the year. Specifically, the rather low economic profitability is due to a low number of TE working hours and an

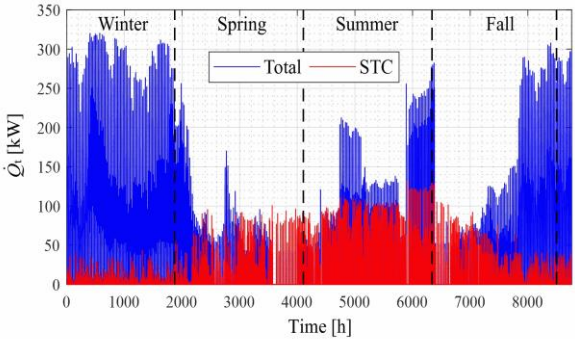

Figure 17. The TES system layout: time history of thermal power demand for NG heating and thermal power supplied by the solar collectors
(*for colour image see journal web site*)

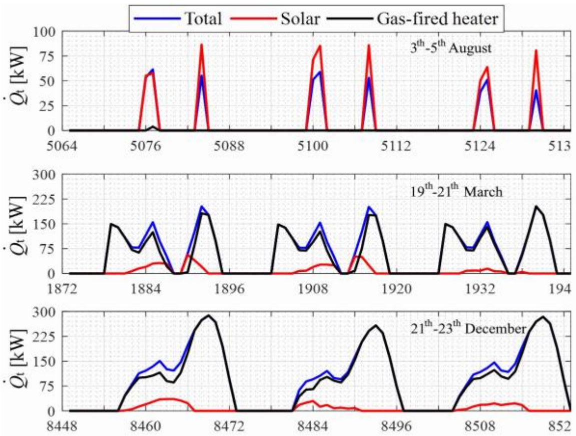

Figure 18. The TES system layout: time history of thermal power demand for NG heating and thermal power supplied by the solar collectors, for three summer, winter and mid-season sample days
(*for colour image see journal web site*)

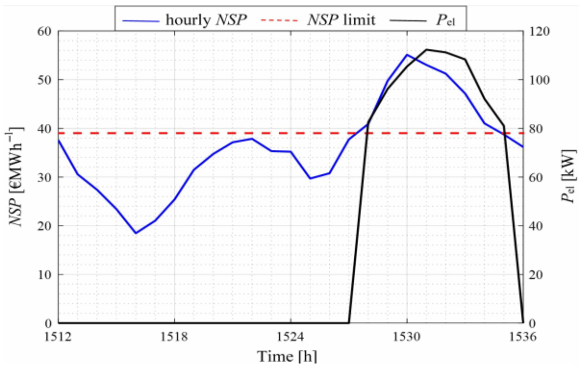

Figure 19. The TES system layout: time history of *NSP* (blue line) and produced electricity power (black line) for a winter sample day (March 4th)
(*for colour image see journal web site*)

averagely low part load ratio of the equipment caused by remarkable NG flow rate fluctuations. Regarding the solar energy collectors, in order to achieve higher savings through their application, PRS with homogeneous NG demands (during both the day and the seasons) are required. From this point of view, an example is represented by PRS feeding industrial users.

Table 5. Yearly energy results for TES and TEV system layouts (constraint for the TE running: minimum allowed NG flow rate and NSP)

	Unit	TES	TEV
The TE working hours	hy^{-1}	3075	2588
Flow rate at PRS	Sm^3y^{-1}	$11.28 \cdot 10^6$	
Flow rate decompressed by TE	Sm^3y^{-1}	$7.86 \cdot 10^6$	$7.76 \cdot 10^6$
Percentage of flow rate decompressed by TE	%	69.7	68.8
Electricity production	MWh_ey^{-1}	276.2	153.0
Thermal energy demand	MWh_ty^{-1}	313.9	160.4
Primary energy demand	$MWhy^{-1}$	348.8	178.2
Net primary energy demand (with STC)	$MWhy^{-1}$	299.6	141.9
Share of renewable energy	%	14	20
PES	$MWhy^{-1}$	300.8^{*}-257.8^{**}	187.4^{*}-154.5^{**}
Percentage of PES	%	50^{*}-42^{**}	57^{*}-46^{**}
Avoided CO_2	$t_{CO_2}\,year^{-1}$	60.6^{*}-52.2^{**}	37.6^{*}-31.2^{**}

*with solar thermal collectors, **with gas-fired heater

Table 6. Yearly economic results: TES *vs*. TEV system layouts

		TES with heater		TES with STC		TEV with heater		TEV with STC	
	Unit	Sell	Self	Sell	Self	Sell	Self	Sell	Self
TWC	$TOEy^{-1}$	97	118	97	117	53	63	53	62
Profits by TWC	$k€y^{-1}$	9.7	11.5	9.7	11.4	5.3	6.2	5.2	6.1
Incentives for solar energy	$k€y^{-1}$	–		2.3		–		2.3	
Operating costs (NG preheating)	$k€y^{-1}$	10.6	12.6	9.2	10.5	5.5	6.3	4.4	4.8
Gross economic proceed	$k€y^{-1}$	16.1	68.5	15.9	67.9	9.0	45.4	8.9	45.1
Net profit (incentives included)	$k€y^{-1}$	15.2	67.4	18.7	68.7	8.8	45.3	12.9	46.5
Investment	k€	603		634		401		431	
SPB	year	39.7	8.8	33.9	9.2	45.6	8.9	33.4	9.3

Conclusions

This paper presents a dynamic simulation model for the energy performance assessment of the energy recovery by the NG decompression through turbo-expansion systems. The developed dynamic simulation model for the energy, economic and environmental performance analysis allows one to take into account the hourly fluctuation of gas pressure, flow rates as well as electricity selling-price to the grid and eventual incentives provided by the legislation. The presented model is a suitable tool for economic feasibility analyses of such kind of plants.

With the aim to perform a comparative analysis and to show the potentiality of the presented tool, a suitable and comprehensive case study, related to a NG decompression station located in South-Italy is developed. Here, the energy, economic and environmental performance analysis of different turbo-expansion system layouts (also coupled to STC for the NG heating) is presented. Remarkable PES and avoided CO_2 emissions are obtained *vs*. traditional system (in which the same amount of electricity is obtained by the national thermoelectric system). The adoption of STC for the NG preheating is a promising solution. Anyway, the energy savings obtained in the developed case study are quite low because of the rather scarce simultaneity between the solar radiation availability and the NG user demand.

In general, the economic results of NG TE are strongly affected by the related still high initial costs. This condition appears critical especially for medium and small size plants. Regarding the investigated case study, the obtained economic results are negatively influenced by the specific use of the decompression station, dedicated to the NG supply to buildings of a small residential community. Here, the system economic convenience is affected by the related low working hours (limited to certain periods of the year) due to the occurring low and highly fluctuating NG-flow rates (with consequent part load ratios system running). In order to get better economic system performances, more homogeneous pressure drops and gas- flow rates during the year are required (*e. g*. as it is obtained in gas decompression stations for supplying industrial users). For the examined case study, the best results are achieved by exploiting the produced electricity for self-consuming purposes. Here, SPB of about nine years are reached. In case of the produced electricity sold to the grid, higher SPB are obtained also because of the low hourly selling prices offered by the national grid.

Nomenclature

A – area, [m^2]
C – capacity, [kWK^{-1}]
C_i – coefficient for the use of the produced heat
c_p – specific heat, [kJkg^{-1}K^{-1}]
E – energy, [kWh]
F – global efficiency, [–]
f – emission factor
h – enthalpy, [kJkg^{-1}]
I – solar radiation, [Wm^{-2}]
IN – incentives for solar energy, [€y^{-1}]
LHV – lower heating value, [MWhSm^{-3}]
M – mass, [ty^{-1}]
$\dot{m}$ – mass-flow rate, [kgs^{-1}]
k – thermal conductivity, [Wm^{-1}K^{-1}]
P – power, [kW]
p – pressure, [kPa]
$\dot{Q}$ – thermal power, [kW]
S – surface, [m^2]
s – thickness, [mm]
t – time, [hours]
T – temperature, [°C]
$\dot{V}$ – flow rate, [Sm^{3}h^{-1}]

Greek symbols

β – pressure ratio, [–]
ξ – exergy, [kWh]
Δ – variation, [–]
η – efficiency, [–]
θ – hour, [h]
τ – coefficient of durability, [–]

Subscripts/Superscripts

amb – environment
el – electric
g – generation
gas – NG
glob – global
int – integration
is – isentropic
m – mechanical
p – primary
pro – proposed system
ref – reference system
sol – solar
u – useful
w – water

Acronyms

COG – co-generative unit
DIV – diverter
HE – HE
IAM – incident angle modifier
JTV – joule thompson expansion valve
NG – NG
NSP – national single price
PES – primary energy saving
PRS – pression reduction station
SC – solar collectors
STC – solar thermal collectors
TE – turbo-expander
TES – two-stage TE in series
TEV – TE coupled to thermal expansion valve
TOE – tonne of equivalent oil
TWC – tradable white certificates, [TOE]
WH – working hours

References

[1] ***, BP Statistical Review of World Energy, 2016, www.bp.com
[2] Neseli, M. A., *et al.*, Energy and Exergy Analysis of Electricity Generation from NG Pressure Reducing Stations, *Energy Conversion and Management*, *93* (2015), Mar., pp. 109-120
[3] ***, Directive 2003/55/EC, European Parliament and of the Council of 26 June 2003, 2003
[4] Bisio, G., Thermodynamic Analysis of the Use of Pressure Exergy of NG, *Energy*, *20* (1995), 2, pp. 161-167
[5] Pozivil, J., Use of Expansion Turbines in NG Pressure Reduction Stations, *Acta Montanistica Slovaca*, *9* (2004), 3, pp. 258-260
[6] Unar, I., *et al.*, Estimation of Power Production Potential from NG Pressure Reduction Stations in Pakistan Using ASPEN HYSYS, *Mehran Uni. Research Jour. of Eng. & Tec.*, *34* (2015), 3, pp. 1-8
[7] Borelli, D., *et al.*, Energy Recovery From NG Pressure Reduction Stations: Integration with Low Temperature Heat Sources, *Energy Conversion and Management*, *159* (2018), Mar., pp. 274-283
[8] Greeff, I. L., *et al.*, Using Turbine Expanders to Recover Exothermic Reaction Heat-Flow Sheet Development for Typical Chemical Processes, *Energy*, *29* (2004), 12-15, pp. 2045-2060
[9] Mirandola, A., *et al.*, Full Load and Partial Load Performance of Poly-Generation Systems with Gas Expanders and Internal Combustion Engines, *Proceedings*, 24th Intersociety Energy Conversion Engineering Conference, Washington, D. C., USA, 1989
[10] Farzaneh-Gord, M., *et al.*, Feasibility of Accompanying Uncontrolled Linear Heater with Solar System in NG Pressure Drop Stations, *Energy*, *41* (2012), 1, pp. 420-428
[11] Farzaneh-Gord, M., *et al.*, Employing Geothermal HE in NG Pressure Drop Station in Order to Decrease Fuel Consumption, *Energy*, *83* (2015), Apr., pp. 164-176
[12] Ghezelbash, R., *et al.*, Performance Assessment of a NG Expansion Plant Integrated with a Vertical Ground-Coupled Heat Pump, *Energy*, *93* (2015), Part 2, pp. 2503-2517
[13] Badami, M., *et al.*, A Biofuel-Based Cogeneration Plant in a NG Expansion System: An Energetic and Economic Assessment, *Applied Thermal Engineering*, *118* (2017), May, pp. 52-61
[14] Jelodar, M. T., *et al.*, Modeling Turbo-expander Systems, *SIMULATION*, *89* (2013), 2, pp. 234-248
[15] ***, Solar Keymark Certification, UNI EN 12976-2, 2017
[16] Kakac, H. L. S., *et al.*, *HEs: Selection, Rating, and Thermal Design*, CRC Press, Boca Raton, Fla., USA
[17] ***, Italian GSE (Manager Energy Service)
[18] ***, Turbinde S.r.l., www.turbinde.eu
[19] Buonomano, A., *et al.*, Experimental Analysis and Dynamic Simulation of a Novel High-temperature Solar Cooling System, *Energy Conversion and Management*, *109* (2016), Feb., pp. 19-39

Paper submitted: January 9, 2018
Paper revised: March 12, 2018
Paper accepted: March 13, 2018